University of Glasgow

UK
Quantum Technology Hub
Sensors and Timing

University of Strathclyde

JWNC
James Watt Nanofabrication Centre

Sub-4 kHz linewidth distributed feedback lasers at 778.1 nm wavelength for two-photon Rb spectroscopy

Eugenio Di Gaetano, Brendan Keliehor, Paul Griffin, Marc Sorel, Erling Riis, and Douglas J. Paul

INSPIRING
PEOPLE

Motivation

Demanding for compact and low-cost **high-power** and **stable narrow-linewidth laser source** for several applications:

- Metrology
- Quantum (e.g. cold atom)
- Sensing (e.g. LIDAR)
- Telecommunications
- Navigation (e.g. GPS)

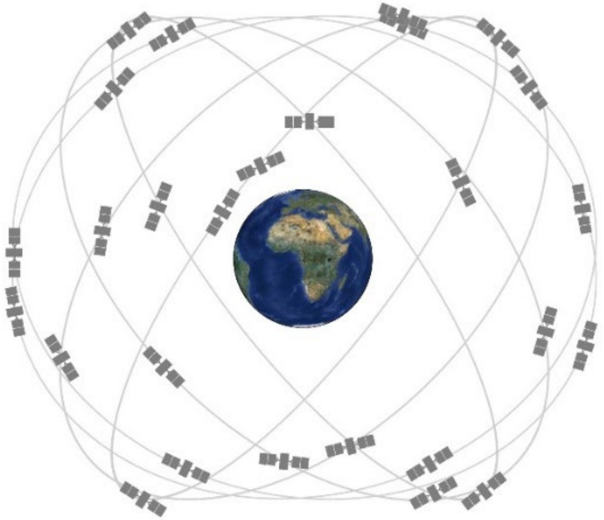

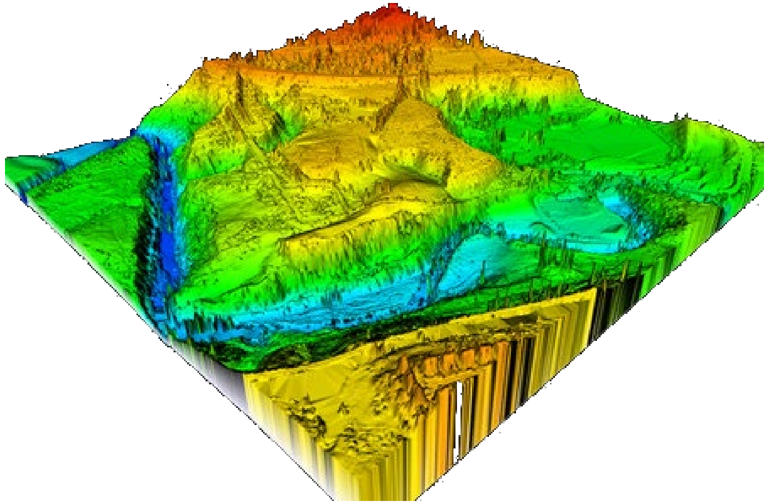

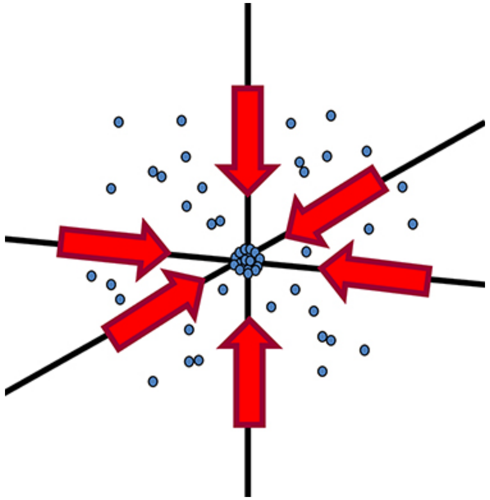

Motivation

Current light sources for quantum applications:

- ☐ Bulky and expensive systems with large power requirements
- ☐ Discrete components prone to environmental misalignment

Advantage of integrated laser sources

- ☐ Reduction in size, production cost, power consumption of 2 order of magnitude
- ☐ On-chip misalignment insensitive and low insertion loss

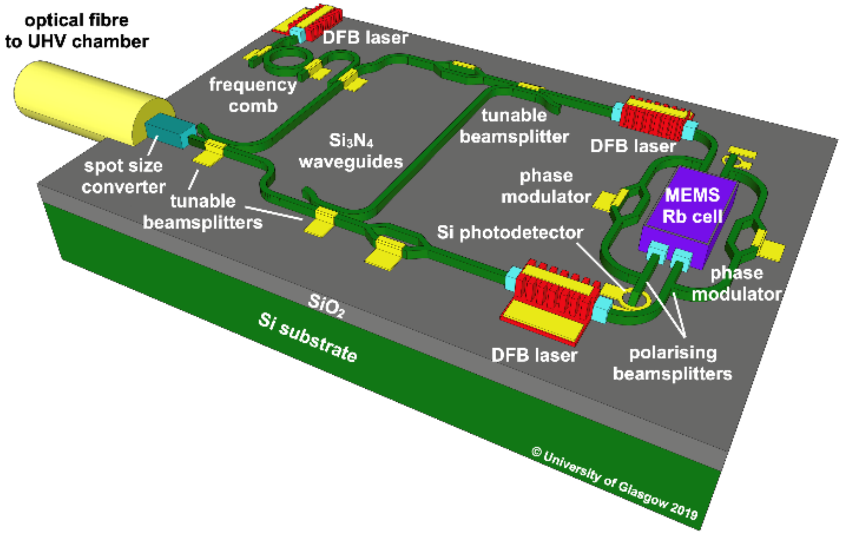

Possible single-chip solution devices

Distributed feedback (DFB) lasers in AlGaAs platform

- ☐ GaAs-AlGaAs platform suitable for emission wavelength in the 700-900 nm wavelength range
- ☐ Single-mode laser emission with narrow linewidth due to the distributed feedback cavity
- ☐ Longitudinal single-mode operation with a side mode suppression ratio (SMSR) exceeding *60dB*
- ☐ Very accurate selection of the emission wavelength by grating pitch and waveguide width

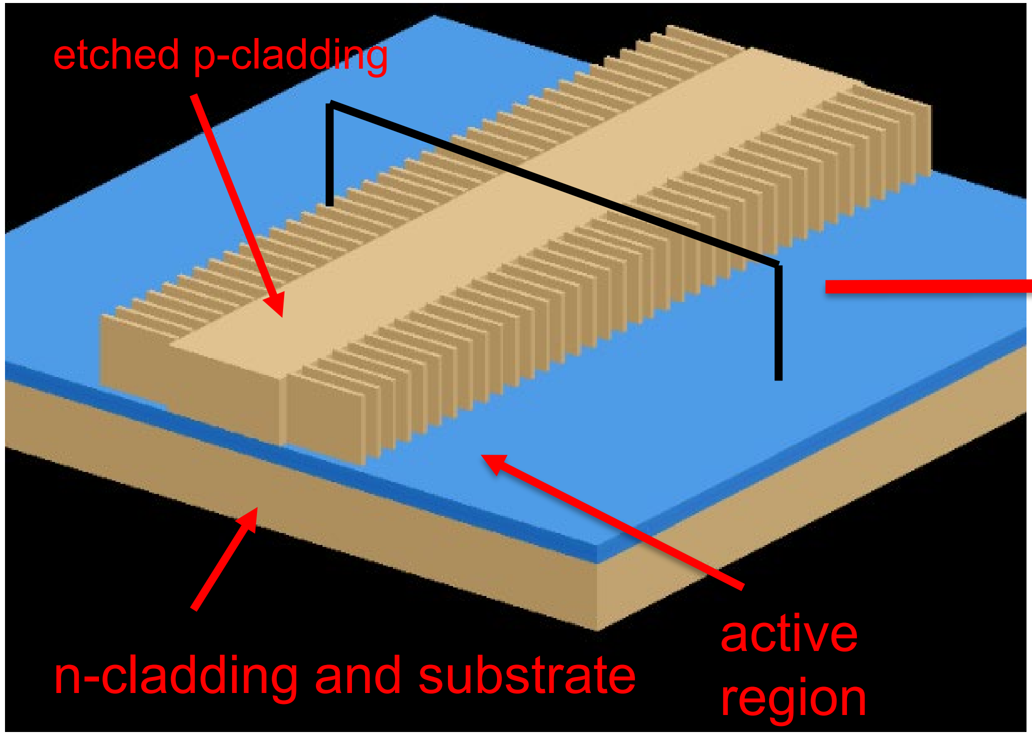

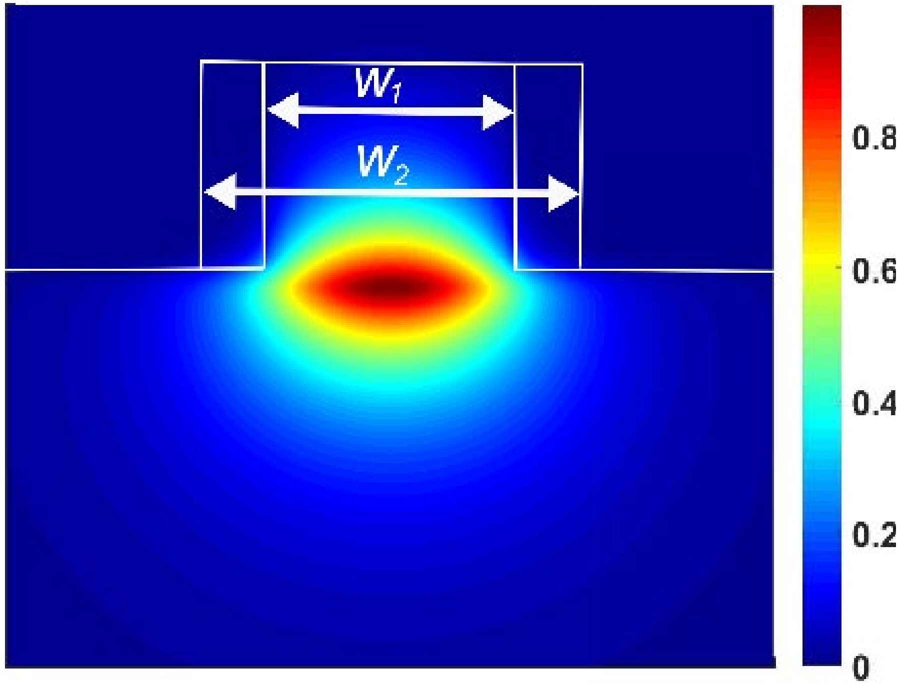

DFB cross section

E. Di Gaetano et al., Opt. Lett. 45, 3529 (2020)

Power and Linewidth in semiconductor laser diodes

In semiconductor lasers the linewidth is described by the Schawlow-Townes formula

$$\Delta\nu = \frac{\Gamma_{QW} R_{spont} h\nu (\alpha_i + \alpha_m)\alpha_m (1 + \alpha_H^2) v_g^2}{8\pi P_{out}}$$

J. Buus, et al., Tunable Laser Diode and Related Optical Sources, 2014

☐ $\boldsymbol{\alpha_i}$ internal losses of the material

☐ $\boldsymbol{\Gamma_{QW}}$ mode confinement in the active region

☐ $\boldsymbol{R_{spont}}$ spontaneous emission rate

☐ $\boldsymbol{\alpha_m}$ feedback losses

☐ $\boldsymbol{P_{out}}$ power output from the laser

☐ $\boldsymbol{\alpha_H}$ linewidth enhancement factor

☐ $\boldsymbol{V_g}$ group velocity

The total power output is proportional to the power density within the laser cavity

$$P_{out} \propto \int_0^L (\overline{P_\perp} \times A(L))\, dL$$

☐ $\boldsymbol{\overline{P_\perp}}$ averaged transversal power density along the laser cavity

☐ ***A*** modal area along the laser cavity

☐ ***L*** longitudinal position along the laser cavity

University of Glasgow

AlGaAs epilayer design

Active region

- ☐ Four 4 nm QWs with photoluminescence around 778 nm
- ☐ Compressive strain QWs for TE emission and parallel bands
- ☐ Aluminium-free InGaAsP quaternary compounds to maximise the power density threshold for catastrophic optical damage

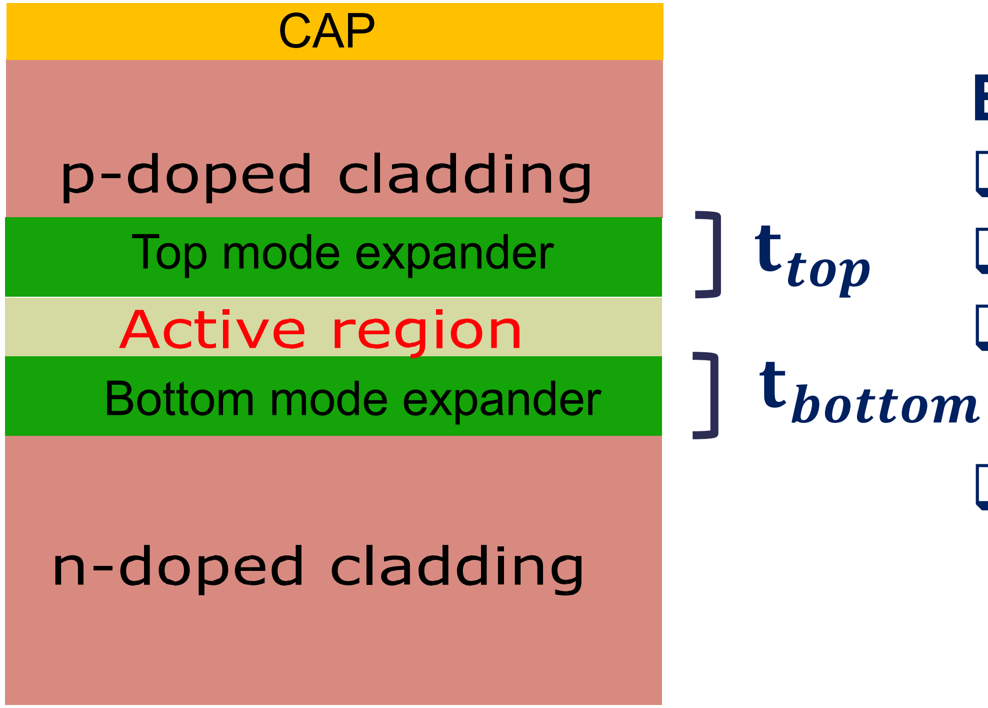

Epilayer optimisation by mode expander to:

- ☐ Increase modal area $\boldsymbol{A}$ to reduce power density
- ☐ Reduce propagation losses $\boldsymbol{\alpha_i}$
- ☐ Reduce modal confinement into the active region $\boldsymbol{\Gamma_{QW}}$
- ☐ Narrow beam emission pattern along the epilayer growth direction

Double-side mode expander design

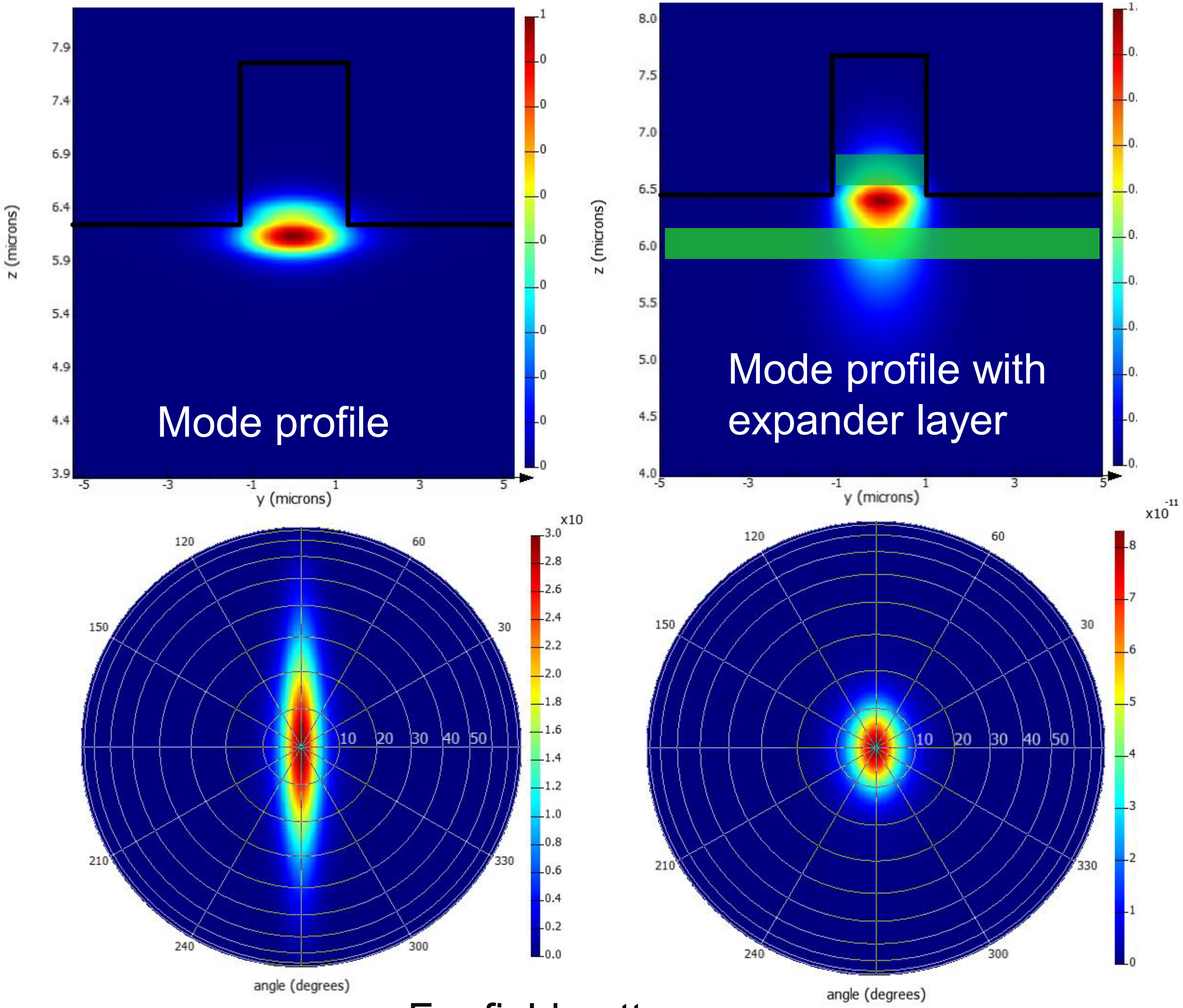

Far field patterns

Double-side mode expander layer makes the mode profile more Gaussian-shaped.

☐ Lower far-field divergence $\boldsymbol{\theta}$ in the epilayer direction

☐ Better coupling components with Gaussian profiles, e.g. lensed optical fibre, and with other PIC components, e.g. SOI or SiN waveguides

☐ Reduce sensitivity to misalignment

Double-side mode expander design

- Modal simulation performed through 2D-FDE solver by Ansys Lumerical considering non-idealies (i.e. RIE lag due to sidewall grating high aspect ratio)

- Trade-off design:
  - decrease laser linewidth Δv
  - reduce power density $\overline{\boldsymbol{P}_{\perp}}$
  - maintain a resonable current density threshold

- Best condition for asymmetrical mode expander with top and bottom thicknesses $0.2\mu\mathrm{m}$ and $2.5\mu\mathrm{m}$, respectively.

- Reduction more than 25%, 70%, 50% for $\boldsymbol{\alpha}_{\mathbf{i}}$, $\boldsymbol{\Gamma}_{QW}$, and $\boldsymbol{\theta}$ Increase more than 400% of $\boldsymbol{A}$

- Relative reduction in linewidth of 18 times, whereas current threshold increase of 14%

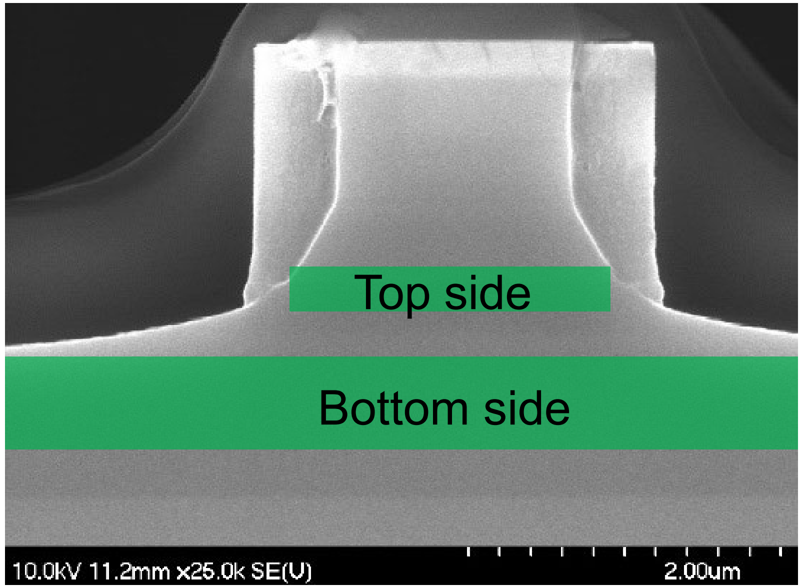

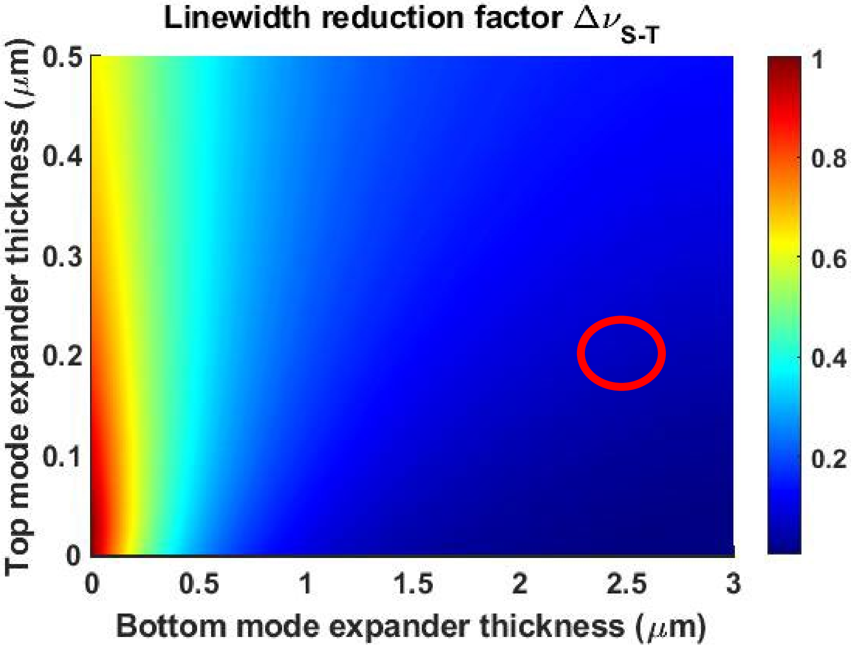

Longitudinal cavity design

- Sidewall DFB waveguide section $\boldsymbol{W_1}, \boldsymbol{W_2}$ selected as 1.5-2.5 $\mu\mathrm{m}$ with a final 5 $\mu\mathrm{m}$-wide adiabatic taper for improved lensed fibre coupling

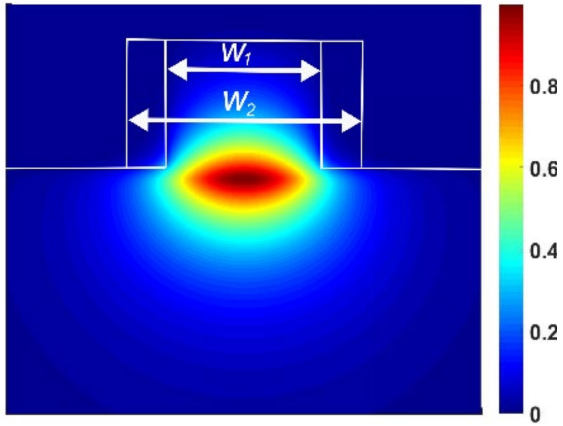

- Total DFB reflectivity depends on the cavity feedback $\boldsymbol{\kappa L}$

$$R = \tanh^2(kL)$$

- Long longitudinal cavity is advantageous:
  1. Increase the cavity feedback $\boldsymbol{\kappa L}$, for fabrication-limited Bragg coupling $\boldsymbol{\kappa}$
  2. Decrease $\overline{\boldsymbol{P}_\perp}$ from same total power
  3. Longer cavity have large $\boldsymbol{\alpha_m}$, so narrower linewidth for the same cavity feedback $\boldsymbol{\kappa L}$

  But longer contact and larger current threshold

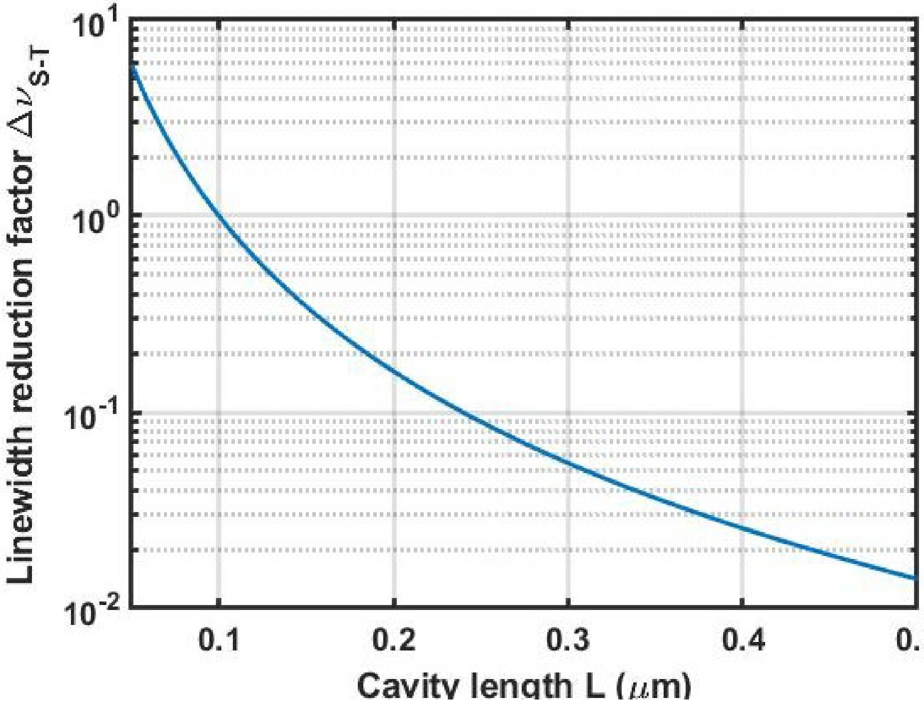

- Cavity length chosen to be **3 mm** long

Fabrication Process

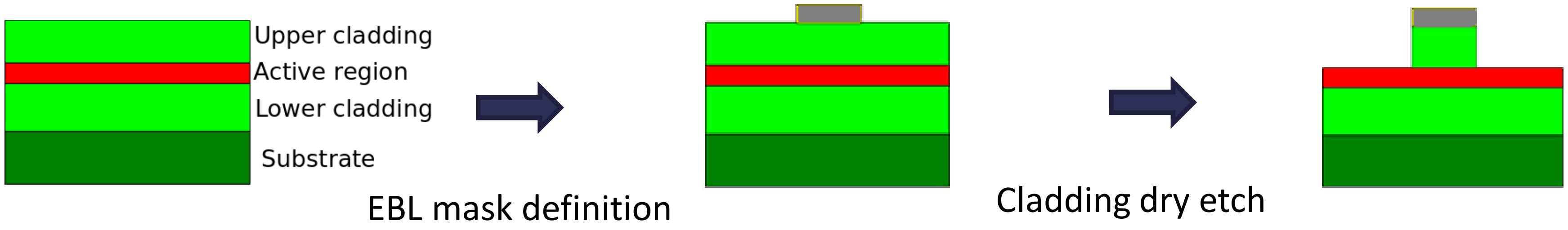

Upper cladding

Active region

Lower cladding

Substrate

EBL mask definition

Cladding dry etch

Critical step: GaAs/AlGaAs dry etch

Lateral view

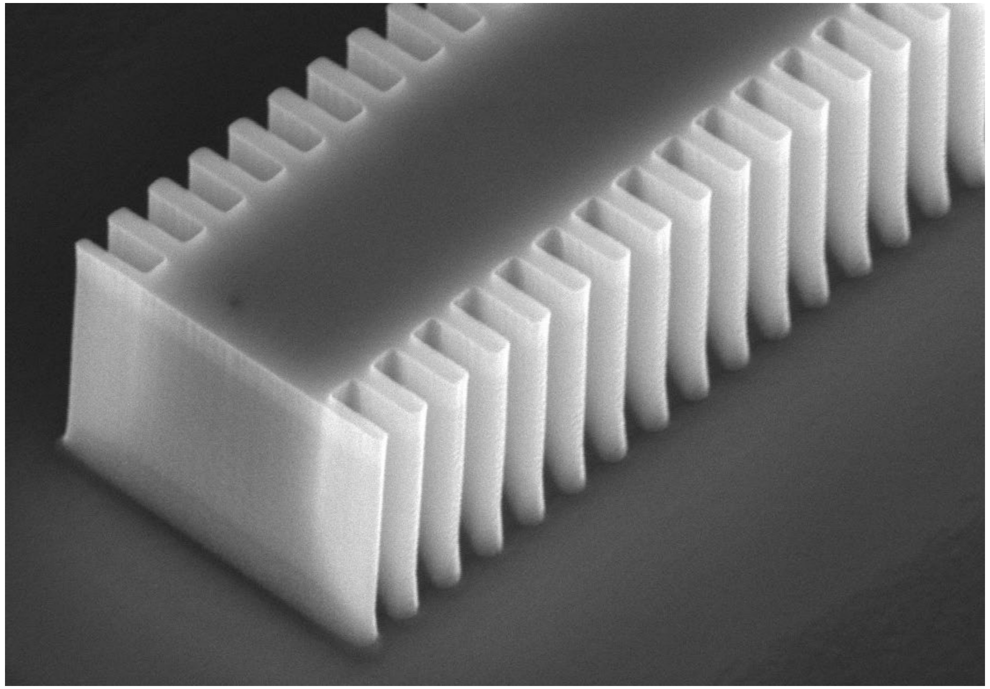

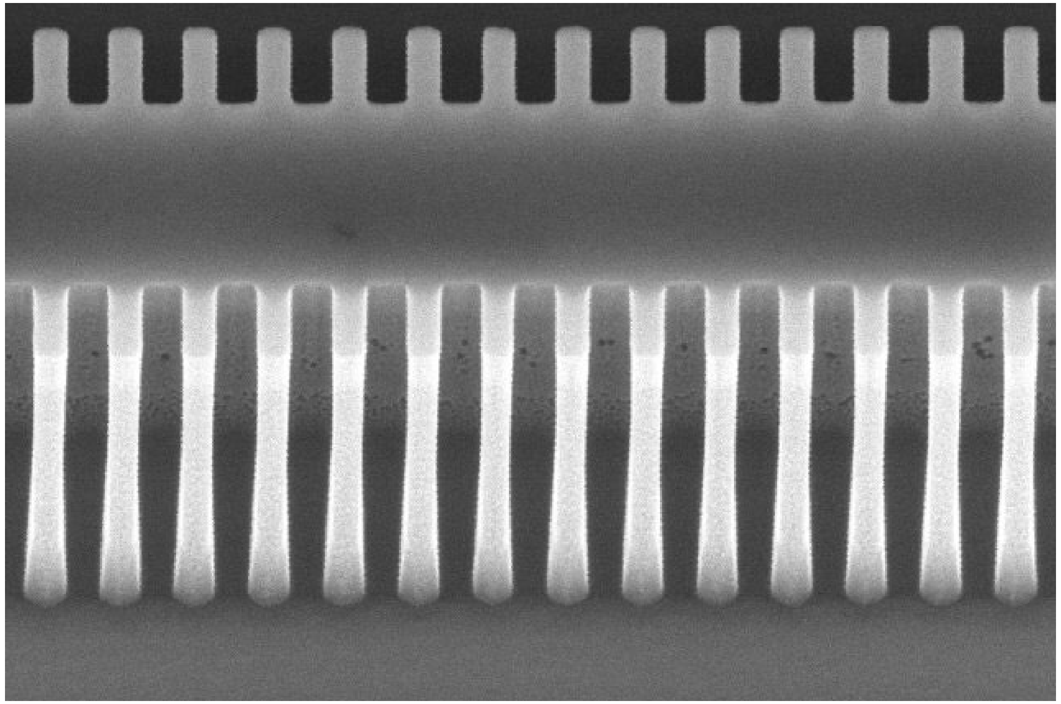

Waveguide end

Smooth sidewall and vertical etch profile are critical to minimise the scattering losses and maximise the Bragg grating coupling κ

Fabrication Process

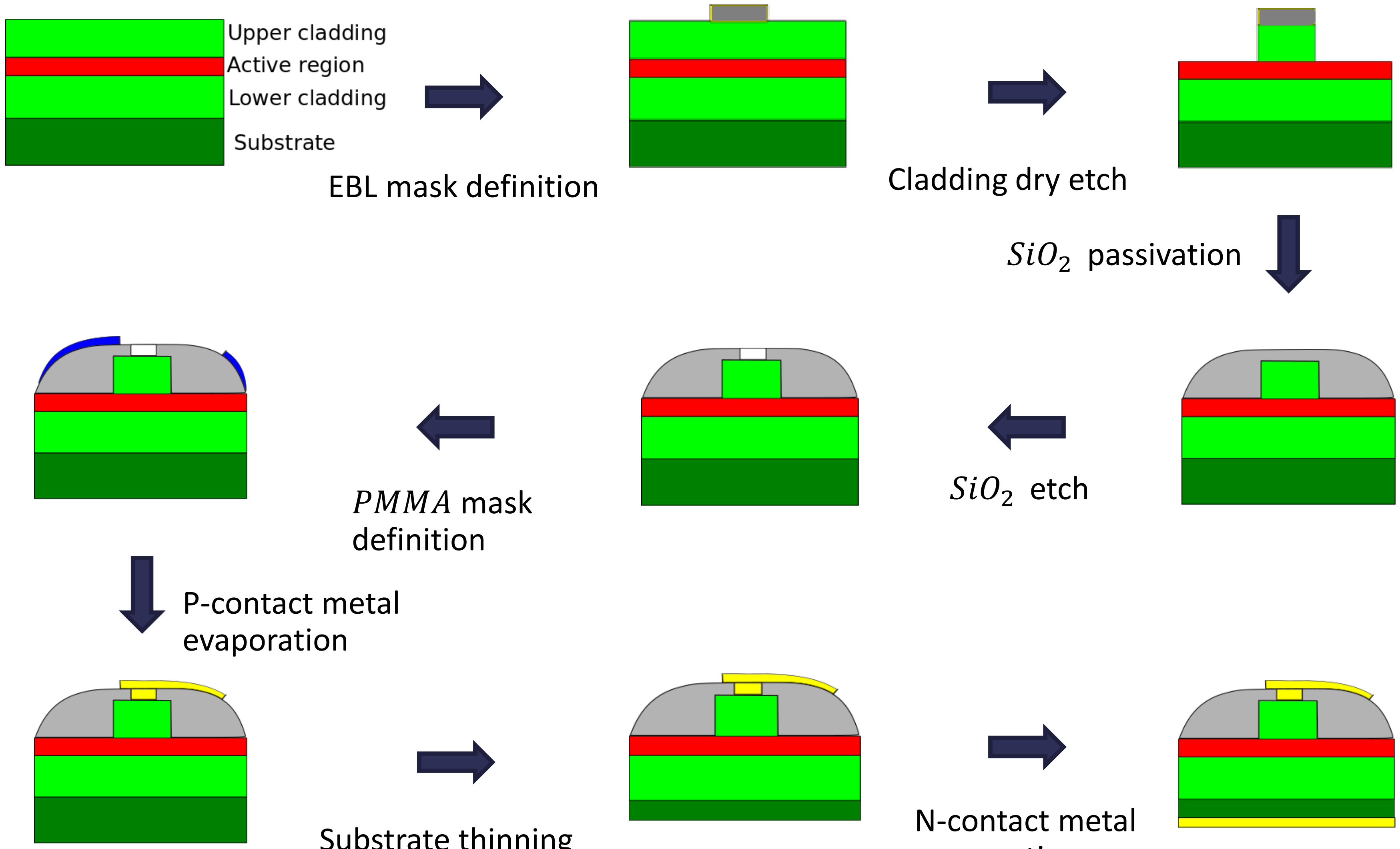

Upper cladding
Active region
Lower cladding
Substrate

EBL mask definition

Cladding dry etch

SiO_2 passivation

SiO_2 etch

$PMMA$ mask definition

P-contact metal evaporation

Substrate thinning

N-contact metal evaporation

High power single-mode lasers

- AR/HR coated facets
- Bar mounted on thermally controlled stage

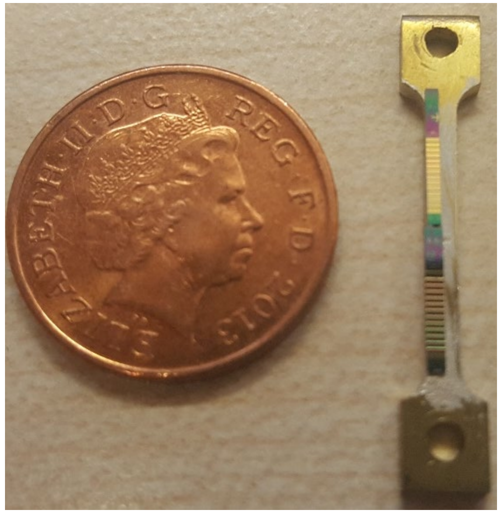

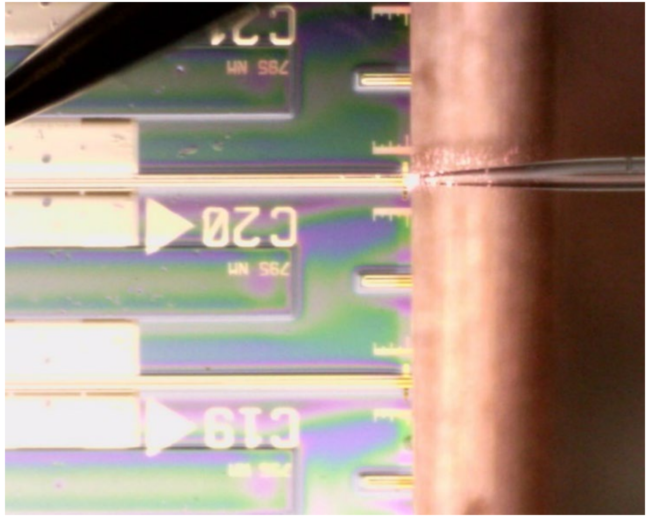

LIV

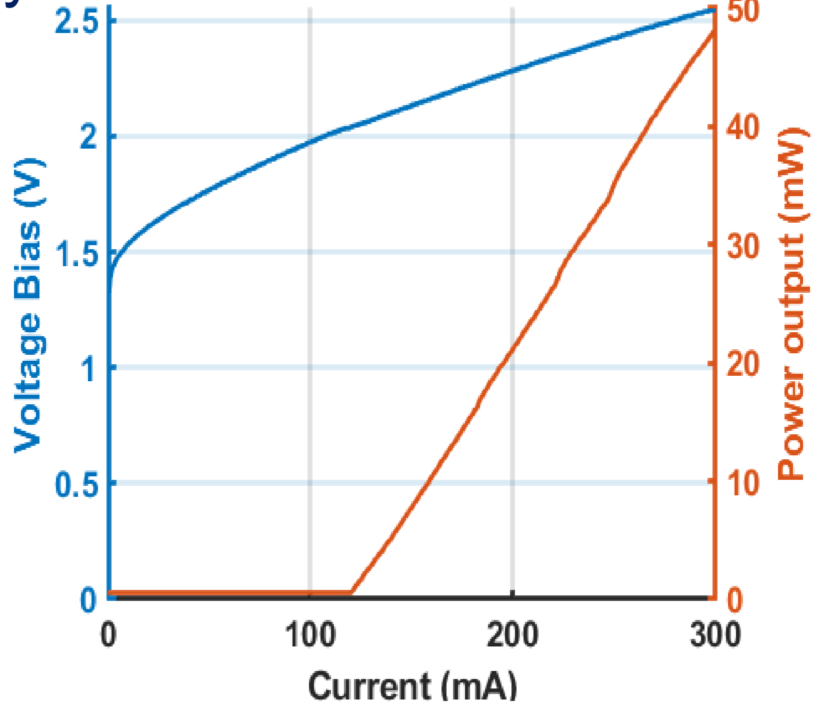

Spectrum

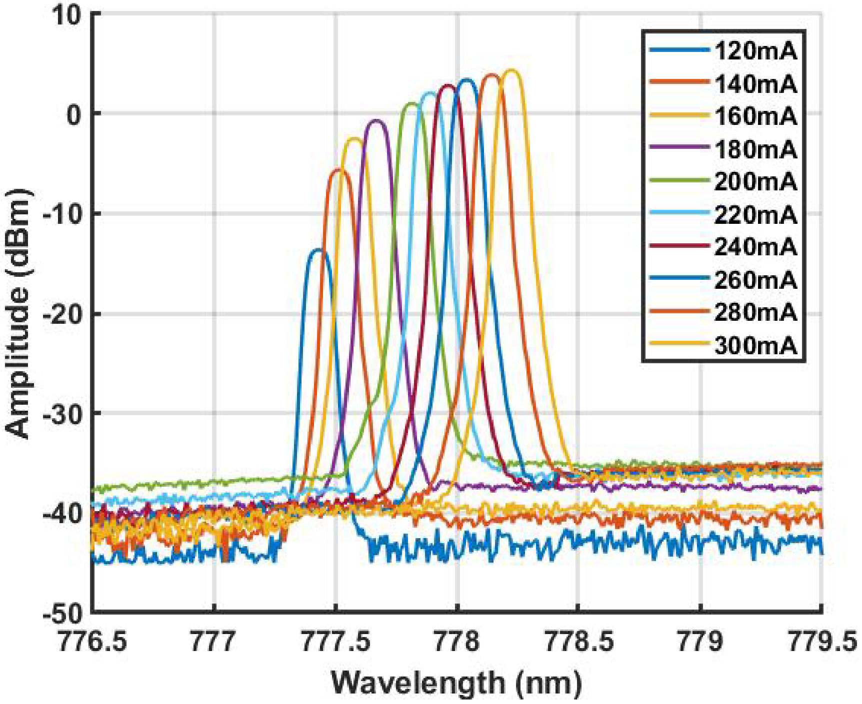

- **Power output exceeding 48 mW**
- **Single-mode emission 778.1 nm**
- **Wavelength tunability range exceeding 0.8 nm**

Far-field pattern characterisation

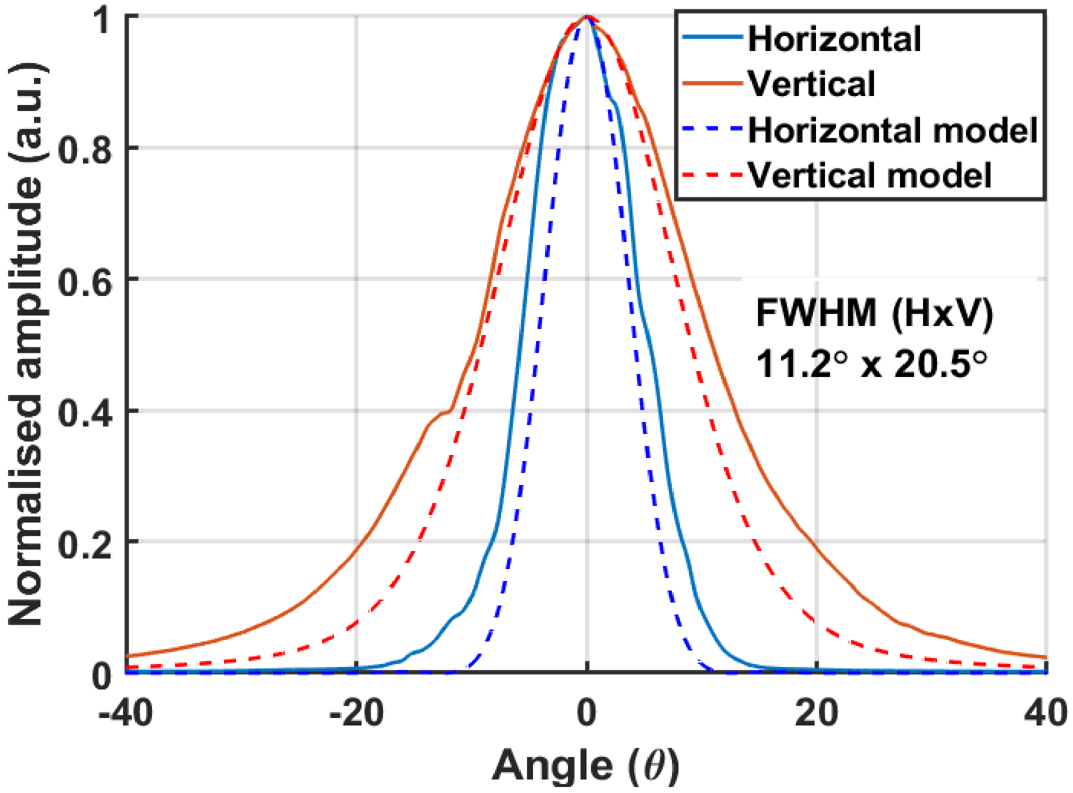

Fibre-coupled LIV

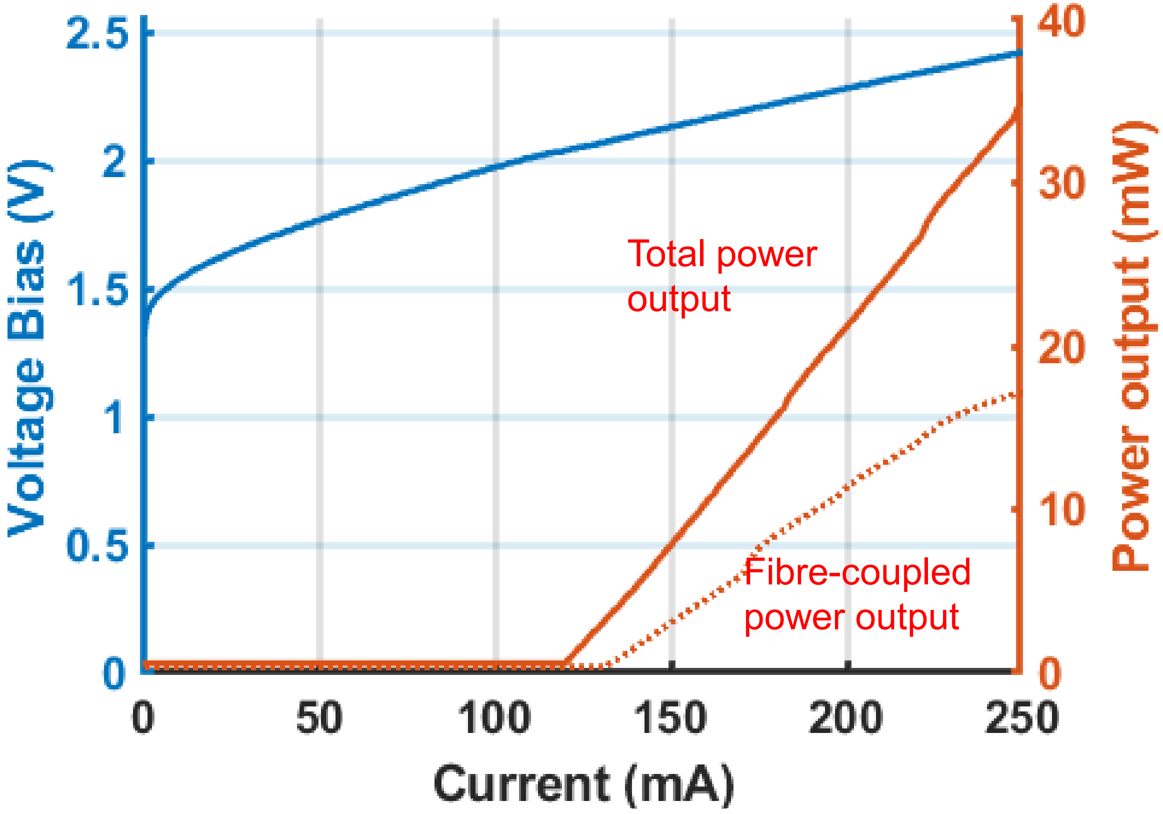

- ❑ Measured pattern far-field pattern confirming model

- ❑ Coupling efficiency as good as 45-50%, improvement of a factor 2 over standard material

RIN and phase noise characterisation

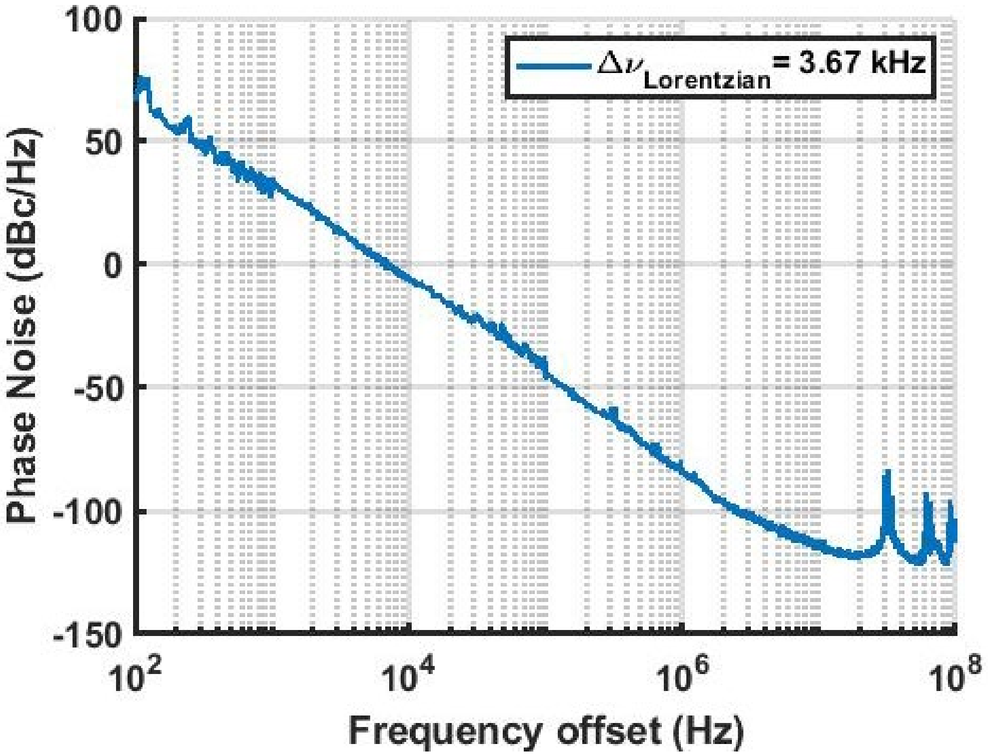

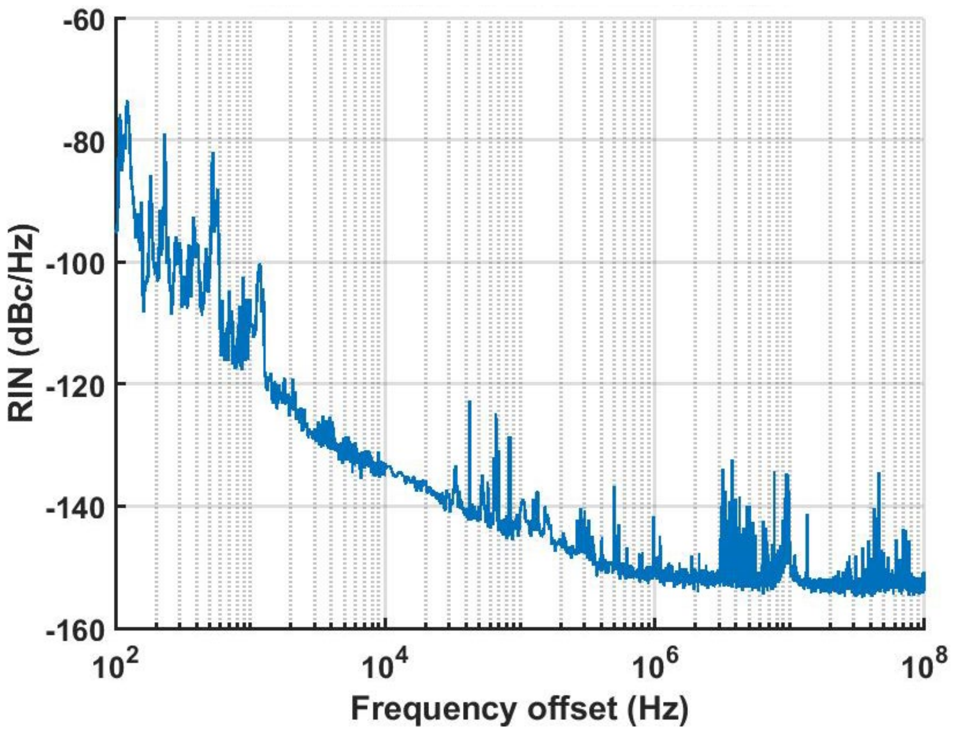

- Lorentizian linewidth as narrow as 3.67 kHz ($\leq 25\mu s$) and 226 kHz for 100 ms integration rime

- RIN as low as -145 dBc/Hz above 100 kHz frequency

Rubidium two-photon spectroscopy: system

Measurement apparatus

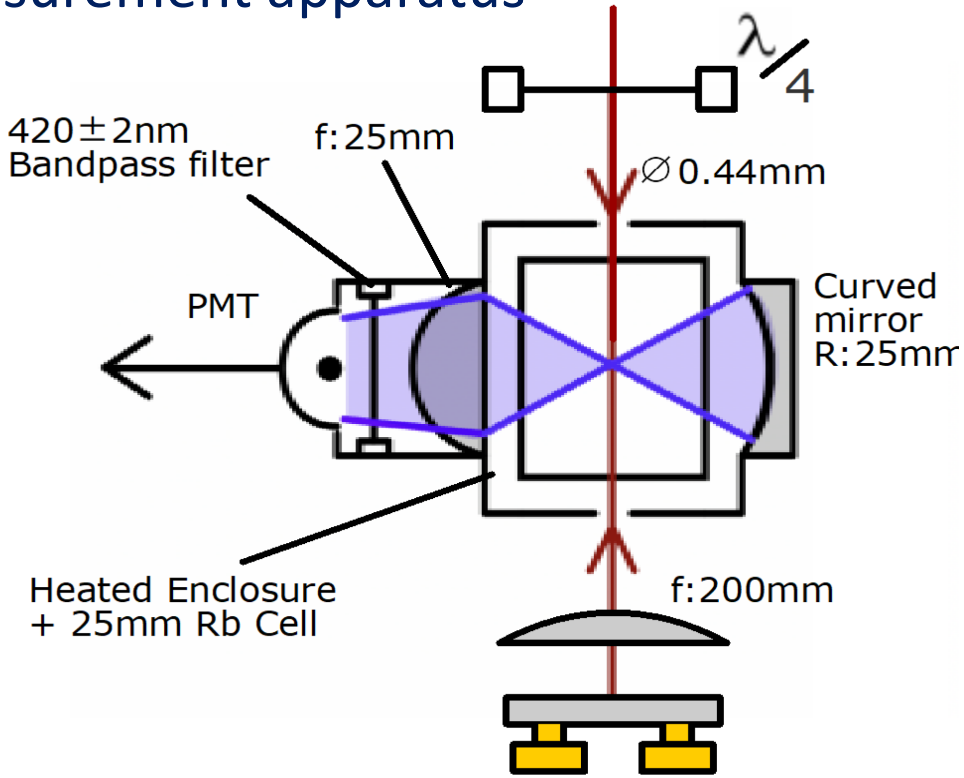

Transition levels for ^{87}Rb two-photon transition

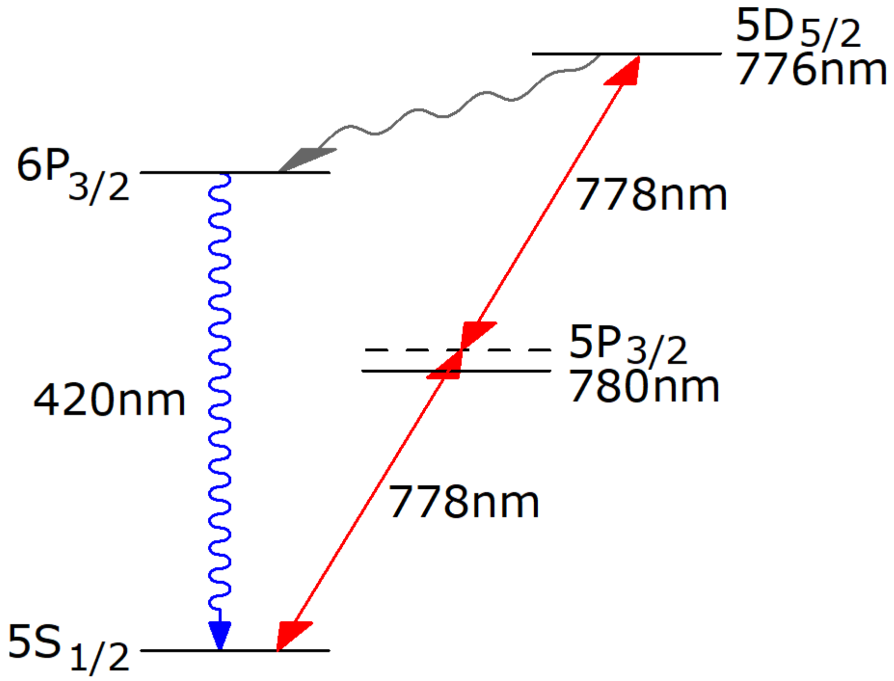

Fluorescence signal hence non-directional emission and weak intensity proportional to:

- Rb atom density, i.e. cell size (25 mm long) and temperature (110 C)
- Laser light intensity ($\propto \mathrm{I}^2$) as two photons are involved

Rubidium two-photon spectroscopy: results

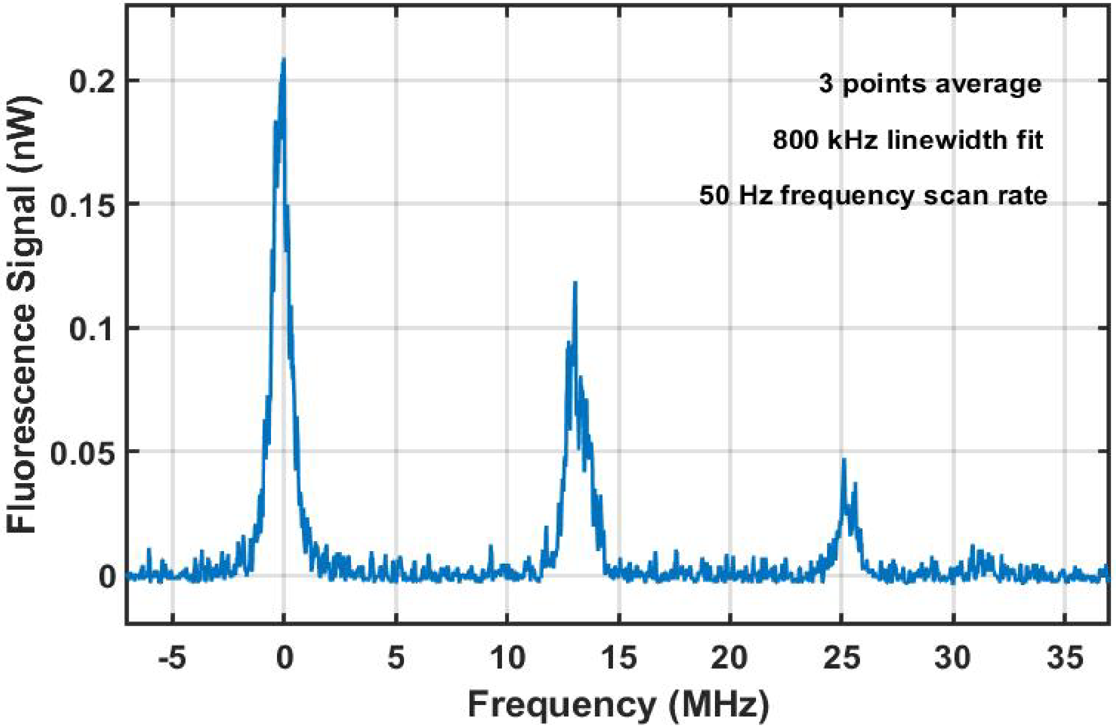

- ☐ Frequency scan around the Rb transitions (55 MHz range) by Acousto-optic modulator with 50 Hz frequency (20 ms scan time)
- ☐ Between 6 - 6.5 mW delivered to the Rb cell for a signal-to-noise between 6 and 10
- ☐ Clear resolution of all the hyperfine levels of the ^{87}Rb two-photon transition

Summary

Achievements

- ☐ Single-mode DFB lasers at 778.1 nm with 48 mW power output, 3.67 kHz Lorentzian linewidth, and RIN = -145 dBc/Hz @ >100 kHz
- ☐ Resolution of ^{87}Rb two-photon transition hyperfine levels in free-running condition

Future developments

- ☐ Improvement of long-time stability by locking on integrated cavity (e.g. SiN microring or Bragg grating)
- ☐ Laser locking onto the ^{87}Rb two-photon transition by Pound-Drever-Hall or other locking techniques

University of Glasgow

Thank you for your attention

Acknowledgement

UK
Quantum Technology Hub
Sensors and Timing

JWNC
James Watt Nanofabrication Centre

ROYAL ACADEMY OF ENGINEERING

University of Strathclyde

UKRI Engineering and Physical Sciences Research Council

UK NATIONAL QUANTUM TECHNOLOGIES PROGRAMME

UKRI Innovate UK